Hydrol. Earth Syst. Sci. Discuss., 9, 595–627, 2012
www.hydrol-earth-syst-sci-discuss.net/9/595/2012/
doi:10.5194/hessd-9-595-2012

Hydrology and Earth System Sciences Discussions

Adaptive correction of deterministic models to produce accurate probabilistic forecasts

P. J. Smith[1], K. Beven[1], A. Weerts[2], and D. Leedal[1]

[1]Lancaster Environment Centre, Lancaster University, UK
[2]Deltares, P.O. Box 177, 2600 MH Delft, The Netherlands

Received: 19 December 2011 – Accepted: 27 December 2011 – Published: 11 January 2012

Correspondence to: P. J. Smith (p.j.smith@lancs.ac.uk)

Published by Copernicus Publications on behalf of the European Geosciences Union.

Abstract

This paper considers the correction of deterministic forecasts given by a flood forecasting model. A stochastic correction based on the evolution of an adaptive, multiplicative, gain is presented. A number of models for the evolution of the gain are considered and the quality of the resulting probabilistic forecasts assessed. The techniques presented offer, in certain situations, an effective and computationally efficient method for providing probabilistic forecasts based on existing flood forecasting system output.

1 Introduction

The basis of many operational hydrological forecasting systems are process based models producing deterministic forecasts. Often significant resources have been invested in acquiring these models and users are familiar with their use and limitations. In many situations such models produce biased or inaccurate predictions of discharge or water level (Aronica et al., 1998; Pappenberger et al., 2007). This makes the issuing of accurate and reliable flood forecasts challenging.

Data assimilation (DA) has been used to address this challenge in two ways: assimilating observations to improve the process model predictions and assimilating observations to improve the representation of the prediction errors. Human forecasters widely practise both forms of DA. Manually altering the internal states of the model based on their interpretation of recent model forecast errors may act to improve future model predictions. The forecaster may use their knowledge of the recent prediction errors of the model in deciding when to issue flood warnings, thereby implicitly utilising the second type of DA. The effectiveness and consistency (across forecasters) of such manual DA techniques is rarely reported formally (Seo et al., 2009).

These manual DA techniques can be formalised to produce deterministic assimilation schemes (e.g. Cole et al., 2009; Moore, 2007). The DA process can also be cast in a probabilistic framework with the aim of constructing the predictive distribution

HESSD

9, 595–627, 2012

$P\left(y_{t+f}|\boldsymbol{y}_{1:T}\right)$ of the observation of some quantity of interest (e.g. water level or discharge) f time steps ahead given $\boldsymbol{y}_{1:T} = (y_1, \ldots, y_T)$ the observations of that quantity up to the current time t.

If the aim of the DA is to improve the predictions of a hydrological model $\mathcal{M}$ a common framework (e.g. Liu and Gupta, 2007) is to cast the model in state space form so that the hydrological states (indexed by time) $\boldsymbol{s}_t$ evolve according to:

$$\boldsymbol{s}_{t+1} = \mathcal{M}(\boldsymbol{s}_t, \boldsymbol{u}_t, \varepsilon_t) \tag{1}$$

where the $\boldsymbol{u}_t$ are observed extraneous inputs (e.g. precipitation) and ε_t a stochastic noise. The model states are then related to the observed values by the observation function $\mathcal{H}$ and stochastic noise ζ_{t+1}:

$$y_{t+1} = \mathcal{H}(\boldsymbol{s}_{t+1}, \zeta_{t+1}). \tag{2}$$

The stochastic term ε_t may be additive, that is

$$\boldsymbol{s}_{t+1} = \mathcal{M}(\boldsymbol{s}_t, \boldsymbol{u}_t) + \varepsilon_t.$$

It may also act within $\mathcal{M}$ to represent a number of features such as noise on the forcing term $\boldsymbol{u}_t$ or time evolving model parameters (e.g. Rajaram and Georgakakos, 1989). By correcting the states of the model it may be hoped that predictions derived for unobserved sites (such as the internal nodes of a hydraulic model) may also be improved. This of course cannot be validated until observations are taken at these points.

The operational usefulness of the predictive distribution constructed from the above state space formulation is dependant upon:

- an appropriate description of the distributions of ε_t and ζ_t;
- an adequate solution of the filtering problem inherent in producing the forecasts.

Addressing both of these topics introduces a number of barriers to the operational implementation of this technique.

HESSD
9, 595–627, 2012

If either $\mathcal{M}$ or $\mathcal{H}$ is non-linear the solution to the filtering problem is not trivial. Approximate solutions to the filtering problem can be provided by a number of algorithms such as particle filters (e.g. Doucet et al., 2001; Moradkhani et al., 2005a; Weerts and El Serafy, 2006), non-linear extensions to the Kalman Filter (Rajaram and Georgakakos, 1989; DaRos and Borga, 1997; Evensen, 2003; Moradkhani et al., 2005b; Reichle et al., 2008) or variational techniques (Li and Navon, 2001; Madsen and Skotner, 2005; Seo et al., 2003).

Particle filters, which approximate the desired distributions through Monte-Carlo sampling, can be considered the most flexible, although the computational burden can be large (Smith et al., 2008) and implementation difficult when ε_t dominates the observation noise (Liu and Chen, 1998). The remaining techniques require less computational resource but introduce assumptions such as unbounded distributions that may require careful reparameterisation of the hydrological model if the states are to remain hydrologically interpretable, e.g. volumes of water in the river channel must be greater or equal to zero.

All the techniques outlined above make multiple calls to the process model at each time step. The computational cost of this may be prohibitive for applications in real time when the lead times required for decisions about warnings are a constraint. This is particularly true if the implementation of the filtering algorithm is achieved by providing code that "wraps" the hydrological model and interacts by altering the initial state and parameter files (Weerts et al., 2010).

Regardless of the computational technique utilised great care should be taken in constructing the description of ε_t and ζ_t (Beven et al., 2008; Kirchner, 2006), particularly if there may be systematic biases, including phase errors, in the data or model (Reichle, 2008). The validation of these choices may require the re-analysis of a significant number of historic events, itself time consuming.

Using DA to improve the forecasts of the difference between the hydrological model and observed data can often be performed at minimal computational cost. If a suitable historic record of model output is maintained, the computational cost of setting

Discussion Paper | Discussion Paper | Discussion Paper | Discussion Paper |

HESSD

9, 595–627, 2012

Adaptive correction of deterministic models

P. J. Smith et al.

Title Page
Abstract Introduction
Conclusions References
Tables Figures
◀I ▶I
◀ ▶
Back Close
Full Screen / Esc

Printer-friendly Version

Interactive Discussion

up the DA may also be minimal. A wide variety of stochastic models have been proposed. These range from the classical auto-regressive moving average (ARMA) time series models of Box and Jenkins (1994) used operationally in the UK (Moore, 2007) to more complex semi-parametric methods (e.g. Krzysztofowicz and Maranzano, 2004; Maranzano and Krzysztofowicz, 2004).

To provide reliable forecasts (in the pragmatic and probabilistic sense) these formulations and others (e.g. Montanari and Brath, 2004; Weerts et al., 2011; Seo et al., 2006) have to attempt to capture the potentially complex evolution of the model residuals. These residuals may incorporate a systematic or temporally varying bias. Reliance on temporal correlation within the residuals must be tempered by the fact that the correlation may be non-stationary, often being low at key times such as during the rising limbs of hydrographs (Todini, 2008) and much higher during recession periods. Residuals in extreme situations such as floods may also possess characteristics different to the majority of the data. Furthermore, each flood may reveal previously unknown shortcomings in the hydrological/hydraulic model(s) making their residuals difficult to predict. In such situations, it may be useful to utilise robust error models and predictive bounds.

Section 2 outlines a parsimonious stochastic error model for providing probabilistic forecasts at a single observational site. The simplest form of stochastic model presented has been utilised previously for operational flood forecasting (Lees et al., 1994). The generation of the predictive distribution using the linear Kalman filter is presented. Methods for estimating the parameters of the model are discussed in Sect. 3. Section 4 presents an example application using an operational flood forecasting model from the UK. The validity of the assumptions used in parameter estimation is investigated and the usefulness of the uncertainty representations illustrated.

HESSD
9, 595–627, 2012

2 Methodology

This section presents the stochastic error model utilised within this paper and the computation of the predictive distribution. The representation of the stochastic error model and its evolution is outlined in a state space framework giving a natural framework for computing the predictive distribution as a filtering problem.

2.1 Error Model

Recall that $\boldsymbol{y}_{1:T} = (y_1, \ldots, y_T)$ is a vector of T observations indexed by time with corresponding deterministic hydrological/hydraulic model predictions $\boldsymbol{m}_{1:T}$. The observation y_t is then related to the prediction m_t by an adaptive gain g_t and noise term ϵ_t as outlined in Eq. (3).

$$y_t = m_t g_t + \epsilon_t \tag{3}$$

The gain g_t is a time varying correction for the bias in the model forecast and is evolved stochastically according to local level (Harvey, 1989) or generalised random walk (Jakeman and Young, 1984; Young et al., 1989) models.

The simplest local level model considered is a random walk where g_t is given as the sum of its previous value and the stochastic noise η_t. That is

$$g_t = g_{t-1} + \eta_t. \tag{4}$$

This is referred to as the random walk (RW) model. The local linear trend (LLT) model generalises this by introducing the slope d_t which follows a random walk driven by the stochastic noise ξ_t. Thus,

$$g_t = g_{t-1} + d_{t-1} + \eta_t \tag{5}$$
$$d_t = d_{t-1} + \xi_t. \tag{6}$$

In this paper it is assumed that ϵ_t, along with the stochastic noise terms η_t and ξ_t are not correlated with each other or in time. Further they are realisations of unimodal,

HESSD

9, 595–627, 2012

Adaptive correction of deterministic models

P. J. Smith et al.

symmetric, unbounded random variables that can be summarised by their first two moments:

$$
\begin{aligned}
\mathrm{E}[\epsilon_t] &= \mathrm{E}[\eta_t] = \mathrm{E}[\xi_t] = 0 \\
\mathrm{Var}[\epsilon_t] &= \sigma^2 \\
\mathrm{Var}[\eta_t] &= q_\eta \sigma^2 \\
\mathrm{Var}[\xi_t] &= q_\xi \sigma^2.
\end{aligned}
$$

The validity of these assumptions can assessed from the forecast residuals as shown in Sect. 4.

If $q_\eta = q_\xi$ the trend in the LLT model is deterministic, resulting in the deterministic local linear trend (DLLT) model. When q_ξ is zero the slope is fixed and the evolution of the gain becomes a random walk with drift (RWD) model, that is:

$$g_t = g_{t-1} + d + \eta_t.$$

Setting q_η to zero but allowing positive q_ξ results in an integrated random walk trend, referred to as the IRW model. This often results in a smoother adaptation of g_t compared to the RW model outlined in Eq. (4).

The models outlined above for g_t are parsimonious the only unknown parameters other then σ^2 being the values of noise variance ratios q_η and q_ξ. A further level of complexity can be included by incorporating smoothing or damping parameters. Inclusion of such a parameter α in Eq. (4) results in a first order auto regressive (AR) model for the gain:

$$g_t = \alpha g_{t-1} + \eta_t. \tag{7}$$

Inclusion of the smoothing parameters (α and β) in the local linear trend model gives:

$$g_t = \alpha g_{t-1} + d_{t-1} + \eta_t \tag{8}$$

$$d_t = \beta d_{t-1} + \xi_t. \tag{9}$$

HESSD
9, 595–627, 2012

This is referred to as the smoothed local linear trend (SLLT) model. Two special cases of this are the smoothed random walk (SRW) model; in which $\beta = 1$ and $q_\eta = 0$; and the damped trend (DT) model in which $q_\eta = q_\xi$ and $\alpha = 1$. More general and higher order representations are also possible, such as doubly integrated random walks. Exploration of these is beyond the scope of this paper.

All the models outlined can be conveniently expressed in a state space form with state vector $\boldsymbol{x}_t = \left[g_t \; d_t \right]'$ describing the gain (g_t) and its slope (d_t). The state vector evolves according the state transition matrix $\mathbf{F}$ and system noise matrix $\mathbf{G}$ as:

$$\boldsymbol{x}_t = \mathbf{F}\boldsymbol{x}_{t-1} + \mathbf{G}\begin{bmatrix} \eta_t \\ \xi_t \end{bmatrix}. \tag{10}$$

The state vector is related to the observations by

$$y_t = \boldsymbol{h}_t' \boldsymbol{x}_t + \epsilon_t \tag{11}$$

where $\boldsymbol{h}_t = \left[m_t \; 0 \right]'$. The values taken by $\mathbf{F}$ and $\mathbf{G}$ depend upon the model selected. Table 1 outlines the values taken in terms of the matrix forms given in Eq. (12) for the various models considered along with any other parameter constraints.

$$\mathbf{F} = \begin{bmatrix} F_{11} & F_{12} \\ 0 & F_{22} \end{bmatrix} \quad \mathbf{G} = \begin{bmatrix} G_{11} & 0 \\ 0 & G_{22} \end{bmatrix}. \tag{12}$$

Two methods for the estimation of the parameters are presented in Sect. 3. The following sub-section discusses the use of the Kalman filter to generate the expected value and covariance of the predictive distributions.

2.2 Prediction using the Kalman filter

The assumptions regarding the stochastic noise terms presented in Sect. 2.1 are the minimum required for application of the linear Kalman filter (Kalman, 1960). Suppose the distribution of $\boldsymbol{x}_t$ has similar properties to that of the errors with its expected value and variance given by $\hat{\boldsymbol{x}}_t$ and $\sigma^2 \mathbf{P}_t$ (where $\mathbf{P}_t$ is a 2×2 matrix), respectively. The

HESSD
9, 595–627, 2012
Adaptive correction of deterministic models
P. J. Smith et al.

Kalman filter can be used to predict future states and assimilate the observed data as it becomes available.

The one step ahead predictions of the distribution of the states, conditional upon the data up to time t are given by the expected value:

$$\hat{\boldsymbol{x}}_{t+1|t} = \mathbf{F}\hat{\boldsymbol{x}}_{t|t} \tag{13}$$

and variance $\sigma^2\mathbf{P}_{t+1|t}$ where

$$\mathbf{P}_{t+1|t} = \mathbf{F}\mathbf{P}_{t|t}\mathbf{F}' + \mathbf{G}\mathbf{Q}\mathbf{G}'. \tag{14}$$

The noise variance ratio matrix $\mathbf{Q}$ is constructed as

$$\mathbf{Q} = \begin{bmatrix} q_\eta & 0 \\ 0 & q_\xi \end{bmatrix}.$$

The f-step ahead prediction of the states given the information up to time t can be computed by repeated application of Eqs. (13) and (14).

The f-step ahead prediction error $\nu_{t+f|t}$ and prediction variance $\sigma^2\psi_{t+f|t}$ can be computed from the forecast states using:

$$\nu_{t+f|t} = y_{t+f} - \boldsymbol{h}'_{t+f}\hat{\boldsymbol{x}}_{t+f|t} \tag{15}$$

$$\psi_{t+f|t} = 1 + \boldsymbol{h}'_{t+f}\mathbf{P}_{t+f|t}\boldsymbol{h}_{t+f} \tag{16}$$

Evaluation of these expressions requires knowledge of the future predictions of the flood forecasting model.

When a new observation becomes available it can be used to condition the distribution of the gain by updating the mean and covariance using Eqs. (17) and (19).

$$\boldsymbol{k}_{t+1} = \boldsymbol{P}_{t+1|t}\boldsymbol{h}_{t+1}\psi^{-1}_{t+1|t} \tag{17}$$

$$\hat{\boldsymbol{x}}_{t+1|t+1} = \hat{\boldsymbol{x}}_{t+1|t} + \boldsymbol{k}_{t+1}\nu_{t+1|t} \tag{18}$$

$$\mathbf{P}_{t+1|t+1} = \mathbf{P}_{t+1|t} - \boldsymbol{k}_{t+1}\boldsymbol{h}'_{t+1}\mathbf{P}_{t+1|t} \tag{19}$$

HESSD
9, 595–627, 2012

To evaluate the above recursions some initial values for $\hat{\boldsymbol{x}}_{0|0}$ and $\mathbf{P}_{0|0}$ are required. In this paper a representation based on taking a minimal number of extra parameters is used. To this end the expected value of the gain at initialisation is taken to represent an unbiased forecast, that is:

$$\hat{\boldsymbol{x}}_{0|0} = \begin{bmatrix} y_0 m_0^{-1} \\ 0 \end{bmatrix}. \tag{20}$$

A single additional parameter ϖ is introduced to describe the initial variance as:

$$\hat{\mathbf{P}}_{0|0} = \begin{bmatrix} \varpi & 0 \\ 0 & \varpi \end{bmatrix}. \tag{21}$$

A suitable burn-in period (see Sect. 4) is then used before commencing evaluation of the estimation criteria outlined in the following section.

3 Estimation

This section discusses the estimation of the unknown parameter vector θ defined for the models considered in Table 1. Two types of estimation technique are outlined. The first is maximum likelihood estimation based upon the assumption that the prediction errors are independent realisations of Gaussian random variables. This introduces stronger assumptions about the stochastic noise terms than those introduced in Sect. 2.1. The second method, which is based on minimising the sum of squared expected forecast errors, is more heuristic. In both cases the validity of the error assumptions can be assessed. This is discussed along with the the construction of predictive error bounds.

3.1 Gaussian Maximum Likelihood

In Gaussian Maximum Likelihood (GML) estimation the parameters θ are estimated by maximising the likelihood of the f-step ahead predictions when it is believed that $v_{t+f|t}$

HESSD
9, 595–627, 2012

is drawn independently from a zero mean Gaussian distribution with variance $\sigma^2 \psi_{t+f|t}$. Under these assumptions the log likelihood is:

$$l(\theta) = K - \frac{1}{2}\sum_{t=0}^{T-f} \log\left(\sigma^2 \psi_{t+f|t}\right) - \frac{1}{2\sigma^2}\sum_{t=0}^{T-f} v_{t+f|t}^2 \psi_{t+f|t}^{-1} \tag{22}$$

where K is a constant with respect to θ. The maximum likelihood estimate of σ^2 can be computed conditional upon the other parameters in θ as:

$$\hat{\sigma}^2 = \frac{1}{T-f}\sum_{t=0}^{T-n} v_{t+f|t}^2 \psi_{t+f|t}^{-1}. \tag{23}$$

This allows σ^2 to be concentrated out of Eq. (22) leaving (Schweppe, 1965):

$$l\left(\theta \backslash \sigma^2\right) = K - \frac{1}{2}\sum_{t=0}^{T-f} \log\left(\hat{\sigma}^2 \psi_{t+f|t}\right) \tag{24}$$

which is dependant up on the remaining parameters (denoted $\theta \backslash \sigma^2$). This can be numerically optimised to give maximum likelihood parameter estimates of θ.

The uncertainty in the predictions can be expressed as percentile confidence intervals for the predictions constructed as:

$$\boldsymbol{h}'_{t+f} \hat{\boldsymbol{x}}_{t+f|t} \pm \kappa_p \hat{\sigma} \psi_{t+f|t}^{\frac{1}{2}} \tag{25}$$

were κ_p is constant dependant upon p and can be computed from a standard normal distribution; for example $\kappa_{95} \approx 1.96$.

The normality of the forecast residuals and their correlation can be readily assessed using, for example, quantile and auto correlation plots (Box and Jenkins, 1994).

HESSD
9, 595–627, 2012

3.2 Minimising the sum of the squared expected forecast errors

The second estimation technique, referred to as SEFE for the remainder of this paper, is based on the appeal of minimising the sum of the squared expected forecasting error:

$$S_f = \sum_{t=0}^{T-f} v_{t+f|t}^2 . \tag{26}$$

The minimisation of S_f allows the estimation of all the parameters in θ except σ^2. A value for σ^2 can then be estimated using Eq. (23) if required. The error assumptions of the Kalman filter (Sect. 2.1) imply that each predictive distribution is uni-modal, symmetric and unbounded. Testing the symmetry of the forecast residuals, for example using Wilcoxon sign rank test (Wilcoxon, 1945), can indicate if this assumption is valid. Two methods for construction of predictive confidence intervals are considered. They make use of the theoretical symmetry of the forecast distribution and result in symmetric prediction intervals.

The symmetry of the forecast distribution implies that prediction confidence intervals can be expressed as:

$$\boldsymbol{h}'_{t+f} \hat{\boldsymbol{x}}_{t+f|t} \pm \rho_p \psi_{t+f|t}^{\frac{1}{2}} . \tag{27}$$

The values of ρ_p can be estimated empirically as the pth percentile of $\left| v_{t+f|t} \psi_{t+f|t}^{-\frac{1}{2}} \right|$. Given the finite population of residuals this empirical estimate of ρ_p may not be not robust at high values of p. The values of ρ_p can be adapted (for given p) as more data becomes available. Sequential tests for symmetry (e.g. Weed and Bradley, 1971) may be of use in such situations.

HESSD
9, 595–627, 2012

Pukelsheim (1994) gives theoretical results for the upper limits of ρ_p under the unimodel, symmetric and unbounded distributional assumptions. Specifically

$$\Pr\left(\left|\frac{y_t - \mu_{t+f|t}}{\psi_{t+f|t}^{-\frac{1}{2}}}\right| \geq r\right) \leq \frac{4\sigma^2}{9r^2} \quad r > 1.63\sigma. \tag{28}$$

The case $r = 3\sigma$ is the three sigma rule; that there is less then 5 % probability of a sample from univariate random variable random with the aforementioned properties being outside of 3 standard deviations from the mean. These upper limits can be used in two ways. Firstly, they allow for the estimation of conservative prediction confidence intervals, allowing for a more cautious view to be taken of the prediction uncertainty. The second use is as a means of analysing the suitability of the adaptive gain models considered by contrasting the symmetrical empirical estimates and theoretic upper limits of given ρ_p.

4 Upper Severn case study

To illustrate the effectiveness and limitations of the proposed methodology in an operational setting a case study based on the Upper Severn catchment (UK) is presented The Upper Severn river network is situated on the border of England and Wales and shown in Fig. 1. The River Severn rises in the Cambrian mountains (741 mAOD) and flows to the northeast before meeting the Vyrnwy tributary at Crew Green. The valley is wide and flat in this confluence area, with a considerable extent of flood plain. The river then flows east to Shrewsbury. The lower boundary of the 2284 km^2 Upper Severn catchment is defined by the gauge at Welshbridge in Shrewsbury where the median annual flood is greater then 284 cumecs. Average annual rainfall can exceed 2500 mm in the head waters of the catchment. The catchment has seen seven significant flood events in the past twelve years.

HESSD
9, 595–627, 2012

The existing flood forecasting model consists of a number of simplified rainfall-runoff representations linked to an ISIS hydrodynamic model. Results are shown for two sites shown in Fig. 1, Welshbridge the lower boundary of the catchment and Llandrinio an internal node of the hydraulic model at which observations are available. The latter is just upstream of the junction with the major Vrnwy tributary and may be affected by backwater effects at flood stages.

Operationally the flood forecasting model is evaluated twice daily. At midnight it is run in a continuous mode using observed inputs and output data assimilation to generate a set of "warm states" which are used to initialise the forecasts. The first set of forecasts issued at midnight (00:00) give up to 36 h lead time using forecast precipitation. The second set of forecasts is issued at midday (12:00). These forecasts are initialised by evolving the "warm states" using the observed meteorological variables between midnight and midday. Forecast precipitation is then used to evaluate the flood forecasting model giveing forcasts of the hydrological variables with upto 36 h lead time. Further details can be found in Weerts et al. (2011).

The adaptive gain correction is initialised at the start of each forecast period. The first four hours of forecasts are used as a burn-in period for the adaptive gain. Then, in keeping with the operational system, forecasts are issued based on the most recent forecast run of the flood forecasting model for which the adaptive gain is burnt in. A single year of data (2006) which contains a significant flood event is used to identify and estimate the adaptive correction. Three years (2007–2009) are used for validation purposes. The results for each of the sites are summarised below.

4.1 Welshbridge

Figure 2 shows the hydraulic model predictions and observed data at Welshbridge during the calibration period. It can be noted that there is a bias in the estimation of the low water level periods. Such biases often arise when attempting to achieve an acceptable flood forecasting model. The adaptive gain correction could be utilised to correct the forecasts in these low flow periods. The difference in relationship between

HESSD

9, 595–627, 2012

Adaptive correction of deterministic models

P. J. Smith et al.

the hydraulic model and observed data for the low flow periods and when this model is responding to rainfall suggest that a different calibration of the stochastic model for the adaptive gain may be required for each. For flooding purposes the response to rainfall is more important. Therefore the calibration and validation criteria are only evaluated at Welshbridge for the simulations of the hydraulic model which forecast a water level greater then 1 m.

Table 2 summarises the calibration results at various forecast lead times. The calibration using the Gaussian likelihood assumptions shows that those model for the adaptive gain which incorporate smoothing parameters have superior performance to those without. This becomes less marked at longer lead times with the exception of the IRW and DLLT models whose performance deteriorates rapidly. The use of time series identification criteria such as the AIC (Akaike, 1974) or BIC (Schwarz, 1978) leads to the selection of the SLLT or SRW model depending upon the lead time considered.

The results from the SEFE calibration suggest that, with the exceptions of the SRW, IRW and DLLT models, there is little difference in RMSE perfomance at short to medium lead times. At longer lead times the SLLT and AR models return lower RMSE values. For shorter lead times the random walk model may then be preferred due to its parsimony. For both calibration methodologies the DLLT and IRW perform poorly indicating that rate of change of the slope d_t is not smooth or constant.

Figure 3 shows two summary plots of the standardised 6 h forecast residuals of the SLLT model calibrated using the Gaussian likelihood methodology. The upper pane indicates the residual distribution has heavier tails than a standard normal distribution. This is particularly true of the lower tail and is the result of including some low water periods in the calibration. Excluding these suggests that the Gaussian assumption is approximatly valid. The lower plot indicates that the residuals are correlated up to at least a lag of 28 samples, or 7 h, approximately the forecast lead time. This and the low corelation value suggest that the conditional independence assumption, while not strictly valid, may be a reasonable approximation.

The forecast residuals of the SEFE methodology can also be assessed. The lower pane of Fig. 4 shows the auto-correlation pattern in the residuals of the RW model fitted by the SEFE methodology for a 6 h leadtime. The correlation within the residuals is higher and more persistant at longer lags than for the Gaussian calibration. The upper pane of Fig. 4 indicates a lack of symmetry in the residuals confirmed by a Wilcoxon sign rank test.

Table 3 shows the percentage of observations falling within the 95 % prediction confidence interval during the validation period. The high percentages for the Gaussian likelihood calibration at short forecast lead times further supports the suggestion that the assumptions used in deriving the likelihood may not be valid. The results for the SEFE calibration indicate that the symmetrical empirical estimation of ρ_p derived during calibration performs poorly in the validation period. The predictive bounds derived using the theoretical upper limit appear to bracket around 99 % of the data during the validation period, suggesting they are unduly conservative.

Figure 5 shows the predictions made using the SLLT model calibrated using the Gaussian methodology for the largest flood events at Welshbridge in the calibration and validation periods. The results are encouraging with the adaptive gain acting to correct the model forecast towards the observed values. During both the calibration and validation period adaptive gain methodology is able to correct for errors in both the timing and magnitude of the hydrograph peaks as well as the receeding limb. The validation results also reveal one aspect of how the adaptive gain behaves in a less than ideal situation. During January there is a period where no observations are taken. During this time, the prediction interval can as first be seen to gradually widen, as no further observations are available to condition the correction of the current simulation of the flood forecasting model. Then, when the next run of the flood forecasting model becomes availalbe the prediction interval widens since the adaptive gain model is initialised but no observations are avaialable to condition the initial uncertainty about the components of the gain. In such situations the forecaster making operational decisions may wish to consider the past simulation of the flood forecasting model and the

HESSD
9, 595–627, 2012

corresponding adaptive gain.

4.2 Llandrinio

Tables 4 and 5 summarise the performance in calibration and validation of the adaptive gain models at Llandrinio. As at Welshbridge there is a bias in the baseflow of the hydraulic model. Perfomance is assessed only when the flood forecasting model predicts a water level greater than 1.8 m. For all the gain models the performance deteriorates markedly at longer lead times. As for Welshbridge gain models which represent a smooth or constant change in the gain; that is DLLT and IRW models; perform more poorly. Similar analysis to that applied at Welshbridge indicates that, although the assumptions of the likelihood model are not strictly valid, the Gaussian calibration methodology performs much better then the SEFE methodology in validation (Table 5).

One of the main reasons for rapidly decreasing perfomance at longer lead times is highlighted in the upper pane of Fig. 6 where the rising limb of the hydrograph is poorly characterised. In part this is due to difficulties with correctly initialising the adaptive gain when the catchment is reponding to a rainfall event yet the model is still rising from its bias lowflow estimate. This is exacerbated at Llandrinio, compared to Welshbridge, since the response of the catchment to rainfall is much more rapid. This suggests that rapidly changing gain values, caused for example by timing errors between the flood forecasting model and the observed data are much more difficult to capture using this methodology than gradually changing biases.

The lower pane of Fig. 6 highlights the danger of assimilating erroneous observations, which in this case produce a significant bias in the predictive confidence interval at future observations.

HESSD
9, 595–627, 2012

5 Conclusions

The results presented in this paper indicate that comparatively simple error models combined with real time data assimilation can provide useful probabilistic forecasts. The techniques used are not computationally demanding. In an operational setting only the linear Kalman filter evolving two states need be evaluated. Though not discussed this can be readily implemented in spreadsheet packages without recourse to more complex programming. This makes the addition of these data assimilation techniques to existing deterministic forecasting systems very straightforward with a very low "cost of entry".

The results shown are for a medium size river basin. These suggest that the calibration based on the Gaussian maximum likelihood theory, though not satisfying the error assumption used in its derivation, performs well in practice. The results at Llandrinio highlight some difficulties in initialisation of the gain and are generally poorer then those downstream at Welshbridge. It remains to be seen if such a data assimilation methodology is able to perform adequately on small basins where the response to rainfall is more rapid and timing errors, due perhaps to errors in the rainfall forecast, are more severe (though see Alfieri et al., 2011, for some initial results).

Recognising that the gain at different sites may be correlated opens up a further line for future research. If such correlations can be successfully exploited it will both increase the robustness of the data assimilation scheme to missing observations and potentially allow forecast updating at sites where very limited data are available (e.g. locations only observed during the calibration of a hydraulic model). The exploration of such strategies is the subject of on-going research.

Acknowledgements. This work was made possible by the UK Environment Agency project SC080030 Probabilistic Flood Forecasting. P. J. S. is also funded by the IMPRINTS EU FP7 project. D. T. was also funded by the UK Flood Risk Management Research Consortium.

HESSD

9, 595–627, 2012

References

Akaike, H.: New Look At Statistical-model Identification, IEEE T. Automat. Contr., AC19, 716–723, 1974. 609

Alfieri, L., Smith, P. J., Thielen-del Pozo, J., and Beven, K. J.: A staggered approach to flash flood forecasting case study in the Cévennes region, Adv. Geosci., 29, 13–20, doi:10.5194/adgeo-29-13-2011, 2011. 612

Aronica, G., Hankin, B., and Beven, K.: Uncertainty and equifinality in calibrating distributed roughness coefficients in a flood propagation model with limited data, Adv. Water Res., 22, 349–365, 1998. 596

Beven, K., Smith, P., and Freer, J.: So just why would a modeller choose to be incoherent?, J. Hydrol., 354, 15–32, 2008. 598

Box, G. E. P. and Jenkins, G. M.: Time Series Analysis: Forecasting and Control, Prentice Hall PTR, 3rd edn., 1994. 599, 605

Cole, S. J., Robson, A., Bell, V., and Moore, R.: Model initialisation, data assimilation and probabilistic flood forecasting for distributed hydrological models., Geophys. Res. Abstr., 11, EGU2009-8048-3, 2009. 596

DaRos, D. and Borga, M.: Adaptive use of a conceptual model for real time flood forecasting, Nord. Hydrol., 28, 169–188, 1997. 598

Doucet, A., de Freitus, N., and Gordon, N.: An introduction to Sequential Monte Carlo Methods, in: Sequential Monte Carlo Methods in Practice, edited by: Doucet, A., de Freitus, N., and Gordon, N., chap. 1, New York, Springer-Verlag, 3–13, 2001. 598

Evensen, G.: The Ensemble Kalman Filter: theoretical formulation and practical implimentation, Ocean Dynam., 53, 343–367, 2003. 598

Harvey, A.: Forecasting, Structural Time Series Models and the Kalman Filter, Cambridge University Press, Cambridge, 1989. 600

Jakeman, A. J. and Young, P. C.: Recursive Filtering and Smoothing Procedures For the Inversion of Ill-posed Causal Problems, Utilitas Mathematica, 25, 351–376, 1984. 600

Kalman, R.: A new approach to linear filtering and prediction problems, J. Basic Eng. T.-ASME, 82, 35–45, 1960. 602

Kirchner, J. W.: Getting the right answers for the right reasons: Linking measurements, analyses, and models to advance the science of hydrology, Water Resour. Res., 42, W03S04, doi:10.1029/2005WR004362, 2006. 598

HESSD

9, 595–627, 2012

Adaptive correction of deterministic models

P. J. Smith et al.

Krzysztofowicz, R. and Maranzano, C. J.: Hydrologic uncertainty processor for probabilistic stage transition forecasting, J. Hydrol., 293, 57–73, 2004. 599
Lees, M. J., Young, P. C., Ferguson, S., Beven, K. J., and Burns, J.: An adaptive flood warning scheme for the River Nith at Dumfries, in: 2nd Inter-national Conference on River Flood Hydraulics, edited by: White, W. R. and Watts, J., Wiley, Chichester, 1994. 599
Li, Z. J. and Navon, I. M.: Optimality of variational data assimilation and its relationship with the Kalman filter and smoother, Q. J. Roy. Meteorol. Soc., 127, 661–683, 2001. 598
Liu, J. S. and Chen, R.: Sequential Monte Carlo methods for dynamic systems, J. Am. Stat. Assoc., 93, 1032–1044, 1998. 598
Liu, Y. Q. and Gupta, H. V.: Uncertainty in hydrologic modeling: Toward an integrated data assimilation framework, Water Resour. Res., 43, W07401, doi:10.1029/2006WR005756, 2007. 597
Madsen, H. and Skotner, C.: Adaptive state updating in real-time river flow forecasting – a combined filtering and error forecasting procedure, J. Hydrol., 308, 302–312, 2005. 598
Maranzano, C. J. and Krzysztofowicz, R.: Identification of likelihood and prior dependence structures for hydrologic uncertainty processor, J. Hydrol., 290, 1–21, 2004. 599
Montanari, A. and Brath, A.: A stochastic approach for assessing the uncertainty of rainfall-runoff simulations, Water Resour. Res., 40, W01106, doi:10.1029/2003WR002540, 2004. 599
Moore, R. J.: The PDM rainfall-runoff model, Hydrol. Earth Syst. Sci., 11, 483–499, doi:10.5194/hess-11-483-2007, 2007. 596, 599
Moradkhani, H., Hsu, K. L., Gupta, H., and Sorooshian, S.: Uncertainty assessment of hydrologic model states and parameters: Sequential data assimilation using the particle filter, Water Resour. Res., 41, W05012, doi:10.1029/2004WR003604, 2005a. 598
Moradkhani, H., Sorooshian, S., Gupta, H. V., and Houser, P. R.: Dual state-parameter estimation of hydrological models using ensemble Kalman filter, Adv. Water Resour., 28, 135–147, 2005b. 598
Pappenberger, F., Beven, K., Frodsham, K., Romanowicz, R., and Matgen, P.: Grasping the unavoidable subjectivity in calibration of flood inundation models: A vulnerability weighted approach, J. Hydrol., 333, 275–287, 2007. 596
Pukelsheim, F.: The 3-sigma-rule, Am. Stat., 48, 88–91, 1994. 606
Rajaram, H. and Georgakakos, K. P.: Recursive parameter estimation of hydrologic models, Water Resour. Res., 25, 281–294, 1989. 597, 598

HESSD
9, 595–627, 2012

P. J. Smith et al.

Reichle, R. H.: Data assimilation methods in the Earth sciences, Adv. Water Resour., 31, 1411–1418, 2008. 598

Reichle, R. H., Crow, W. T., and Keppenne, C. L.: An adaptive ensemble Kalman filter for soil moisture data assimilation, Water Resour. Res., 44, W03423, doi:10.1029/2007WR006357, 2008. 598

Schwarz, G.: Estimating Dimension of A Model, Ann. Stat., 6, 461–464, 1978. 609

Schweppe, F. C.: Evaluation of Likelihood Functions For Gaussian Signals, IEEE T. Inform. Theory, 11, 61–70, 1965. 605

Seo, D. J., Koren, V., and Cajina, N.: Real-time variational assimilation of hydrologic and hydrometeorological data into operational hydrologic forecasting, J. Hydrometeorol., 4, 627–641, 2003. 598

Seo, D.-J., Herr, H. D., and Schaake, J. C.: A statistical post-processor for accounting of hydrologic uncertainty in short-range ensemble streamflow prediction, Hydrol. Earth Syst. Sci. Discuss., 3, 1987–2035, doi:10.5194/hessd-3-1987-2006, 2006. 599

Seo, D. J., Cajina, L., Corby, R., and Howieson, T.: Automatic state updating for operational streamflow forecasting via variational data assimilation, J. Hydrol., 367, 255–275, 2009. 596

Smith, P. J., Beven, K. J., and Tawn, J. A.: Detection of structural inadequacy in process-based hydrological models: A particle-filtering approach, Water Resour. Res., 44, W01410, doi:10.1029/2006WR005205, 2008. 598

Todini, E.: A model conditional processor to assess predictive uncertainty in flood forecasting, International Journal of River Basin Management, 6, 123–137, 2008. 599

Weed, H. D. and Bradley, R. A.: Sequential One-sample Grouped Signed Rank Tests For Symmetry – Basic Procedures, J. Am. Stat. Assoc., 66, 321–326, doi:10.2307/2283930, 1971. 606

Weerts, A. H. and El Serafy, G. Y. H.: Particle filtering and ensemble Kalman filtering for state updating with hydrological conceptual rainfall-runoff models, Water Resour. Res., 42, W09403, doi:10.1029/2005WR004093, 2006. 598

Weerts, A. H., El Serafy, G. Y., Hummel, S., Dhondia, J., and Gerritsen, H.: Application of generic data assimilation tools (DATools) for flood forecasting purposes, Comput. Geosci., 36, 453–463, 2010. 598

Weerts, A. H., Winsemius, H. C., and Verkade, J. S.: Estimation of predictive hydrological uncertainty using quantile regression: examples from the National Flood Forecasting System (England and Wales), Hydrol. Earth Syst. Sci., 15, 255–265, doi:10.5194/hess-15-255-2011,

2011. 599, 608
Wilcoxon, F.: Individual Comparisons By Ranking Methods, Biometrics Bull., 1, 80–83, 1945. 606
Young, P., Ng, C., and Armitage, P.: A Systems-approach To Recursive Economic-forecasting and Seasonal Adjustment, Comput. Math. Appl., 18, 481–501, 1989. 600

HESSD
9, 595–627, 2012

Adaptive correction of deterministic models

P. J. Smith et al.

Table 1. Model considered for the evolution of the gain specified in terms of the state space form in Eq. (12) along with any parameter constraints.

Model	F_{11}	F_{12}	F_{22}	G_{11}	G_{22}	Constraints	Unknwon Parameters θ
RW	1	0	0	1	0	$q_\xi = 0$	$\left(\sigma^2, q_\eta\right)$
LLT	1	1	1	1	1		$\left(\sigma^2, q_\eta, q_\xi\right)$
DLLT	1	1	1	1	1	$q_\eta = q_\xi$	$\left(\sigma^2, q_\eta\right)$
RWD	1	1	1	1	0	$q_\xi = 0$	$\left(\sigma^2, q_\eta\right)$
IRW	1	1	1	0	1	$q_\eta = 0$	$\left(\sigma^2, q_\xi\right)$
AR	α	0	0	1	0	$q_\xi = 0$	$\left(\alpha, \sigma^2, q_\eta\right)$
SLLT	α	1	β	1	1		$\left(\alpha, \beta, \sigma^2, q_\eta, q_\xi\right)$
SRW	α	1	1	0	1	$q_{\eta'} = 0$	$\left(\alpha, \sigma^2, q_\xi\right)$
DT	1	1	β	1	1	$q_\eta = q_\xi$	$\left(\beta, \sigma^2, q_\eta\right)$

HESSD
9, 595–627, 2012

Table 2. Calibration results for Welshbridge showing the log likelihood and RMSE (bracketed) for various forecast lead times and GRW models.

	2	6	9	12	18	24
RW	20835.30 (0.08)	11997.89 (0.18)	8912.81 (0.25)	7428.73 (0.31)	6736.32 (0.36)	6311.21 (0.42)
LLT	21141.29 (0.07)	11737.83 (0.18)	8496.08 (0.25)	7175.45 (0.30)	6491.85 (0.35)	6036.23 (0.41)
DLLT	20948.38 (0.09)	11137.46 (0.21)	7635.90 (0.28)	5265.25 (0.32)	3362.42 (0.37)	1747.25 (0.43)
RWD	20809.24 (0.07)	11730.53 (0.18)	8496.09 (0.25)	7175.45 (0.31)	6491.85 (0.36)	6036.23 (0.41)
IRW	20946.31 (0.09)	11137.10 (0.21)	7635.72 (0.28)	5262.32 (0.32)	3353.63 (0.37)	1736.39 (0.43)
AR	20868.70 (0.08)	12084.28 (0.18)	9044.89 (0.24)	7581.42 (0.29)	6855.06 (0.34)	6417.59 (0.39)
SRW	21913.09 (0.09)	12323.80 (0.20)	9392.21 (0.27)	8116.53 (0.30)	6610.70 (0.40)	6100.62 (0.45)
DT	21918.88 (0.07)	12339.99 (0.17)	9047.37 (0.24)	7448.73 (0.30)	6747.79 (0.35)	6332.88 (0.40)
SLLT	21962.31 (0.07)	12447.34 (0.17)	9138.63 (0.24)	7607.88 (0.29)	6908.54 (0.33)	6428.87 (0.38)

HESSD
9, 595–627, 2012

Table 3. Fraction of observations at Welshbridge bracketed by the estimated 95 % prediction intervals during validation. Bracketed results are those for the SEFE calibration with the italicised and bold values corresponding to the empirical and theoretical symmetric bounds.

	2	6	9	12	18	24
RW	0.96 (*0.59*, **0.99**)	0.94 (*0.67*, **0.98**)	0.94 (*0.68*, **0.98**)	0.93 (*0.77*, **0.98**)	0.93 (*0.79*, **0.98**)	0.93 (*0.79*, **0.98**)
LLT	0.97 (*0.59*, **0.99**)	0.94 (*0.67*, **0.98**)	0.94 (*0.67*, **0.98**)	0.93 (*0.78*, **0.98**)	0.93 (*0.79*, **0.98**)	0.93 (*0.79*, **0.98**)
DLLT	0.99 (*0.67*, **1.00**)	0.95 (*0.81*, **0.99**)	0.94 (*0.85*, **0.98**)	0.93 (*0.82*, **0.98**)	0.93 (*0.82*, **0.98**)	0.93 (*0.81*, **0.98**)
RWD	0.97 (*0.59*, **0.99**)	0.94 (*0.67*, **0.98**)	0.94 (*0.68*, **0.98**)	0.93 (*0.78*, **0.98**)	0.93 (*0.80*, **0.98**)	0.93 (*0.79*, **0.98**)
IRW	0.99 (*0.78*, **1.00**)	0.95 (*0.81*, **0.99**)	0.94 (*0.85*, **0.98**)	0.93 (*0.82*, **0.98**)	0.93 (*0.82*, **0.98**)	0.93 (*0.81*, **0.98**)
AR	0.96 (*0.59*, **0.99**)	0.94 (*0.63*, **0.98**)	0.94 (*0.65*, **0.98**)	0.93 (*0.76*, **0.99**)	0.93 (*0.81*, **0.99**)	0.93 (*0.83*, **0.99**)
SRW	0.99 (*0.77*, **1.00**)	0.95 (*0.81*, **0.99**)	0.94 (*0.84*, **0.98**)	0.93 (*0.82*, **0.98**)	0.93 (*0.86*, **0.99**)	0.93 (*0.89*, **0.99**)
DT	0.99 (*0.54*, **0.99**)	0.95 (*0.63*, **0.98**)	0.94 (*0.65*, **0.98**)	0.93 (*0.78*, **0.98**)	0.93 (*0.79*, **0.98**)	0.93 (*0.79*, **0.98**)
SLLT	0.99 (*0.51*, **0.99**)	0.95 (*0.59*, **0.99**)	0.94 (*0.62*, **0.98**)	0.93 (*0.77*, **0.99**)	0.93 (*0.81*, **0.99**)	0.93 (*0.83*, **0.99**)

HESSD
9, 595–627, 2012

Table 4. Calibration results for Llandrinio showing the log likelihood and RMSE (bracketed) for various forecast lead times and GRW models.

	2	6	9	12	18	24
RW	−1061.42 (0.36)	−4744.76 (0.77)	−5479.30 (0.87)	−5697.52 (0.93)	−6391.88 (1.03)	−6419.32 (1.07)
LLT	−1092.91 (0.36)	−4824.86 (0.78)	−5534.55 (0.88)	−5710.48 (0.93)	−6395.27 (1.03)	−6412.10 (1.07)
DLLT	−1443.27 (0.45)	−8904.07 (1.35)	−11 843.91 (1.96)	−14 014.49 (1.50)	−17379.61 (1.59)	−18 990.72 (1.63)
RWD	−1092.91 (0.36)	−4824.76 (0.78)	−5534.55 (0.88)	−5710.48 (0.93)	−6395.27 (1.03)	−6412.10 (1.07)
IRW	−1437.98 (0.47)	−8900.64 (1.35)	−11 848.68 (1.96)	−14 022.42 (1.50)	−17 389.35 (1.59)	−18 966.45 (1.63)
AR	−967.58 (0.36)	−4603.47 (0.75)	−5324.49 (0.84)	−5523.15 (0.89)	−6201.72 (0.97)	−6196.56 (0.99)
SRW	1581.67 (0.42)	−1110.34 (0.69)	−2202.27 (0.80)	−2778.06 (0.85)	−4752.12 (0.94)	−5301.67 (0.98)
DT	1579.94 (0.33)	−1111.16 (0.57)	−2203.04 (0.65)	−2778.85 (0.69)	−4753.57 (0.84)	−5304.04 (0.98)
SLLT	1581.66 (0.32)	−1110.72 (0.58)	−2200.42 (0.65)	−2771.87 (0.69)	−4677.89 (0.94)	−5201.28 (0.98)

HESSD

9, 595–627, 2012

Adaptive correction of deterministic models

P. J. Smith et al.

Table 5. Fraction of observations at Llandrinio bracketed by the estimated 95 % prediction intervals during validation. Bracketed results are those for the SEFE calibration with the italised and bold values corresponding to the empirical and theoretical symmetric bounds.

	2	6	9	12	18	24
RW	0.95 (*0.53*, **0.98**)	0.94 (*0.79*, **0.98**)	0.94 (*0.81*, **0.98**)	0.94 (*0.83*, **0.98**)	0.93 (*0.84*, **0.98**)	0.93 (*0.84*, **0.98**)
LLT	0.96 (*0.53*, **0.98**)	0.94 (*0.80*, **0.98**)	0.94 (*0.81*, **0.98**)	0.94 (*0.83*, **0.98**)	0.93 (*0.84*, **0.98**)	0.93 (*0.84*, **0.98**)
DLLT	0.95 (*0.29*, **0.99**)	0.94 (*0.81*, **0.98**)	0.94 (*0.81*, **0.98**)	0.94 (*0.69*, **0.98**)	0.94 (*0.68*, **0.98**)	0.93 (*0.68*, **0.98**)
RWD	0.96 (*0.53*, **0.98**)	0.94 (*0.80*, **0.98**)	0.94 (*0.81*, **0.98**)	0.94 (*0.83*, **0.98**)	0.93 (*0.84*, **0.98**)	0.93 (*0.84*, **0.98**)
IRW	0.95 (*0.28*, **0.99**)	0.94 (*0.82*, **0.98**)	0.94 (*0.81*, **0.98**)	0.94 (*0.69*, **0.98**)	0.94 (*0.68*, **0.98**)	0.93 (*0.68*, **0.98**)
AR	0.96 (*0.32*, **0.99**)	0.96 (*0.55*, **1.00**)	0.95 (*0.68*, **1.00**)	0.95 (*0.73*, **1.00**)	0.94 (*0.73*, **1.00**)	0.94 (*0.77*, **1.00**)
SRW	0.94 (*0.36*, **0.98**)	0.93 (*0.86*, **0.99**)	0.93 (*0.90*, **0.99**)	0.93 (*0.91*, **0.99**)	0.93 (*0.93*, **0.99**)	0.93 (*0.93*, **0.99**)
DT	0.94 (*0.36*, **0.98**)	0.93 (*0.87*, **0.98**)	0.93 (*0.89*, **0.98**)	0.93 (*0.91*, **0.98**)	0.93 (*0.91*, **0.98**)	0.93 (*0.87*, **0.98**)
SLLT	0.94 (*0.37*, **0.98**)	0.93 (*0.85*, **0.98**)	0.93 (*0.87*, **0.98**)	0.93 (*0.89*, **0.99**)	0.93 (*0.93*, **0.99**)	0.93 (*0.93*, **0.99**)

HESSD
9, 595–627, 2012
Adaptive correction of deterministic models
P. J. Smith et al.

Title Page
Abstract | Introduction
Conclusions | References
Tables | Figures
Back | Close
Full Screen / Esc
Printer-friendly Version
Interactive Discussion

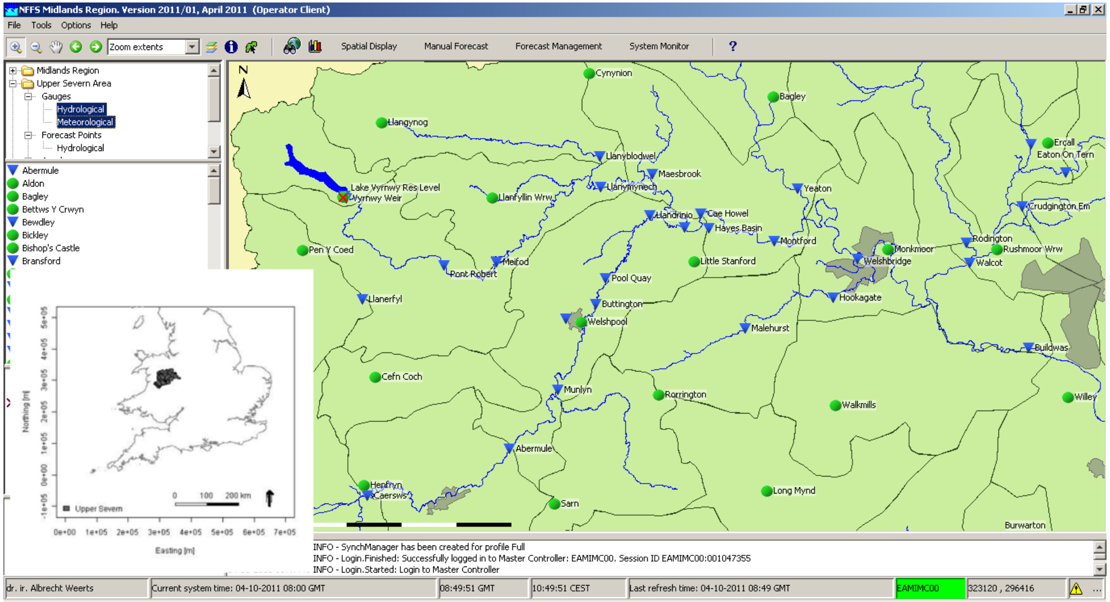

Fig. 1. Screenshot from the UK National flood forecasting system showing the Upper Severn catchment with the forecast sites studied highlighted. The insert shows the location of the catchment within the UK.

HESSD

9, 595–627, 2012

Adaptive correction of deterministic models

P. J. Smith et al.

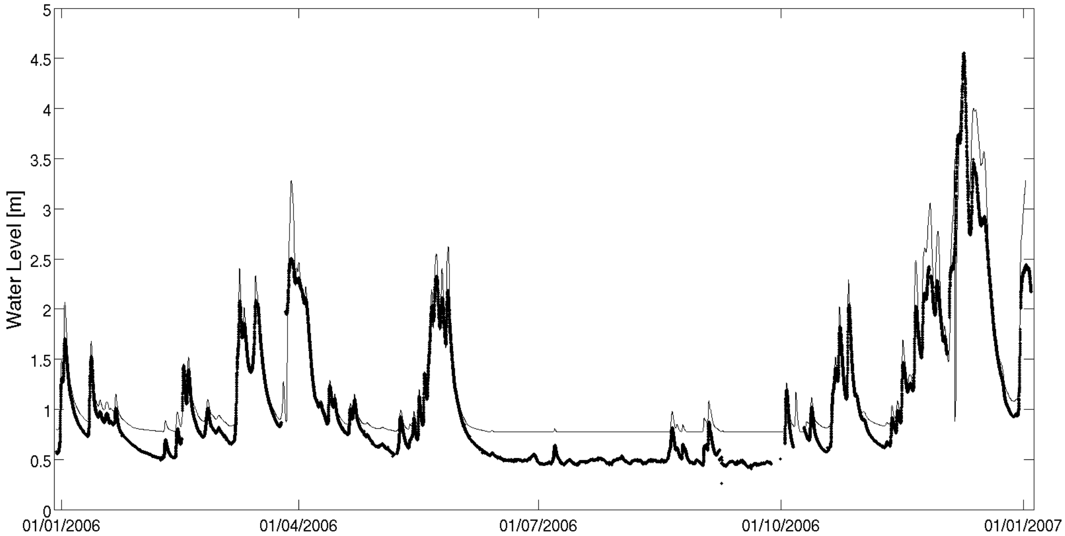

Fig. 2. Summary plots of the data available for Welshbridge during the calibration period. Points represent observed data with the line being the concatenation of the output of the most recent hydraulic model initialisation. A bias in the prediction of low flows is clearly shown as are periods of missing data and poor model initialisation.

HESSD

9, 595–627, 2012

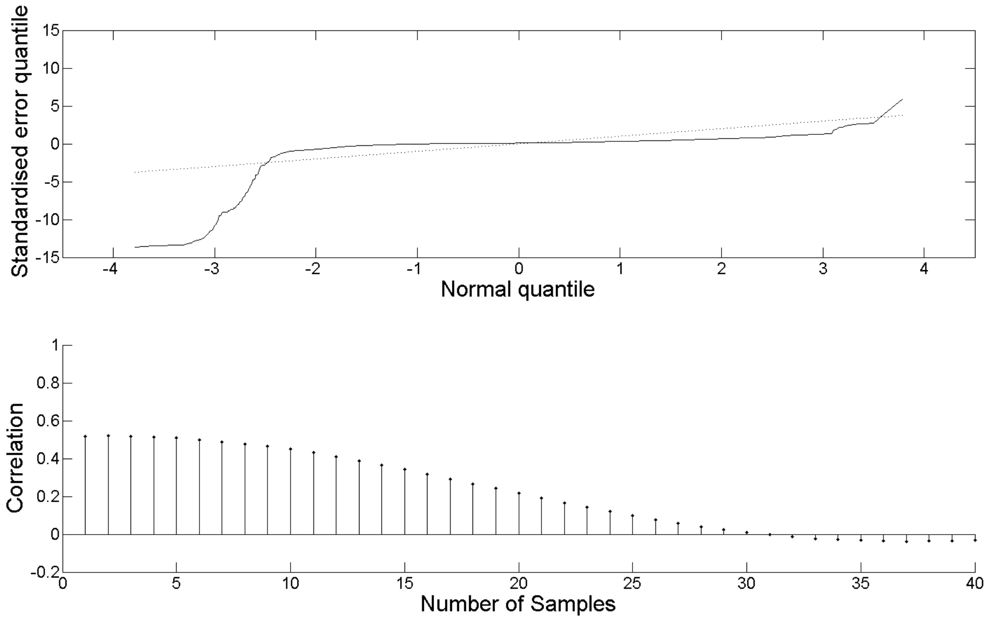

Fig. 3. Summary plots of the analysis of the 6 h forecast residuals for the DT model calibrated using the Gaussian maximum likelihood methodology. The upper pane shows the quantile quantile plot of the standardised residuals compared to a standard normal distribution. The lower pane shows the auto-correlation of the residuals.

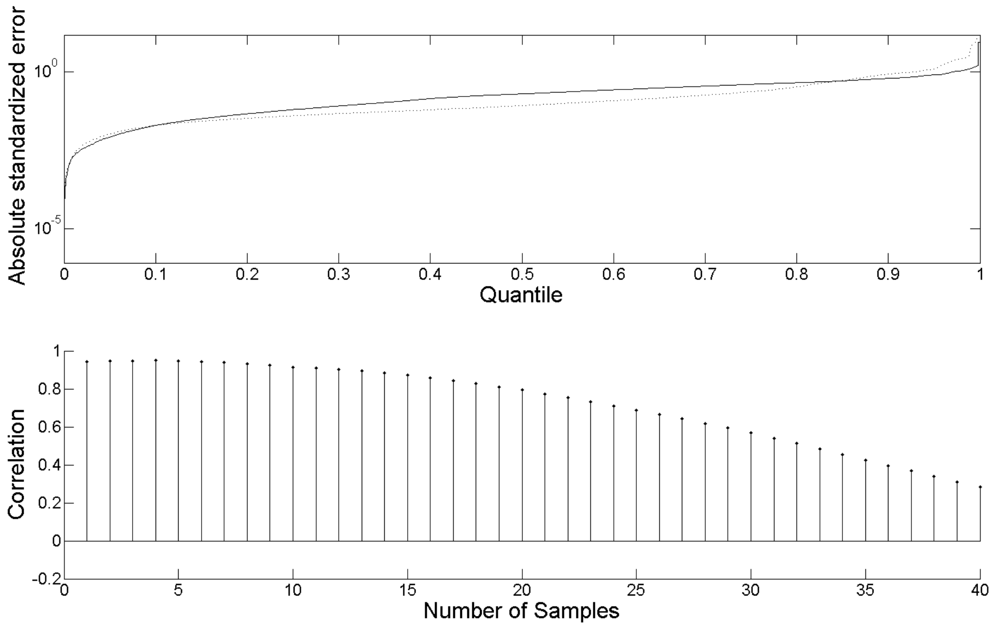

Fig. 4. Summary plots of the analysis of the 6 h forecast residuals for the RW model calibrated using the SEFE methodology. The upper pane shows the quantiles of the absolute values of the residuals. The solid line being positive residuals and the dotted line being negative residuals. The lower pane shows the auto-correlation of the residuals.

HESSD
9, 595–627, 2012

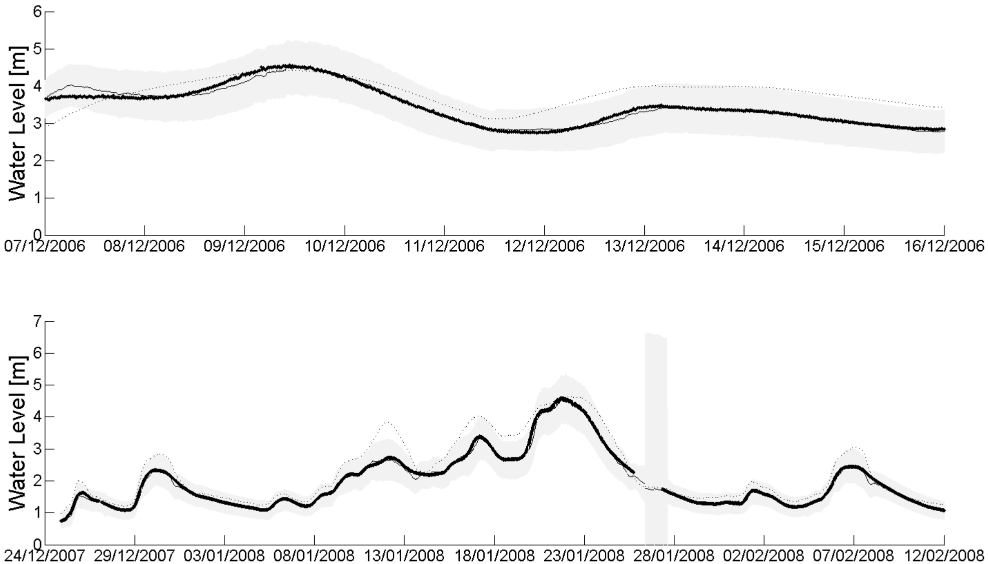

Fig. 5. Examples of 6 h ahead forecasts given at Welshbridge for two large flood events during calibration (upper pane) and validation (lower pane) periods generated using the DT model calibrated using the Guassian methodology. The shaded area represents the 95 % prediction confidence interval with the solid line the expected value of the predictions. Observed data points are also shown.

HESSD
9, 595–627, 2012

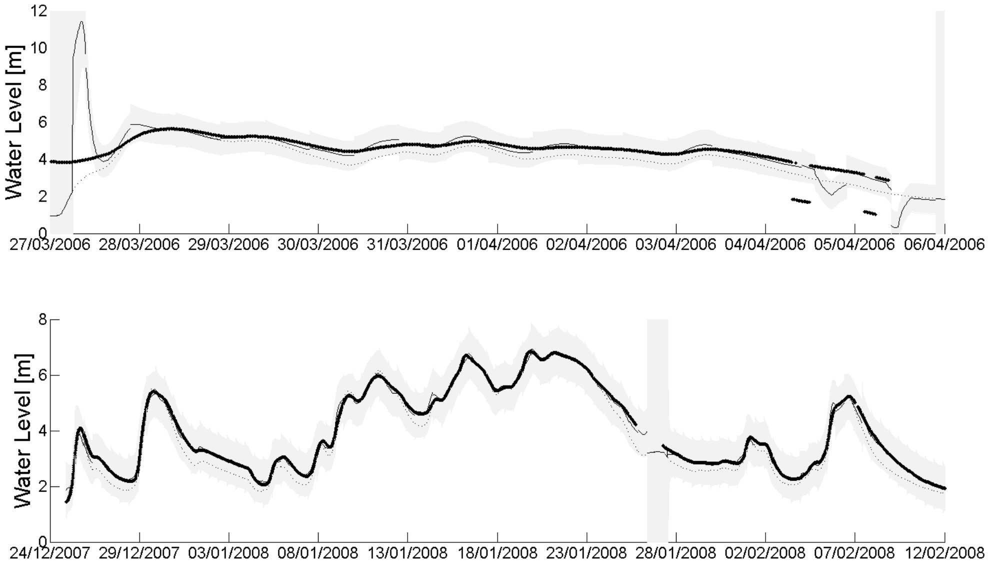

Fig. 6. Examples of 6 h ahead forecasts given at Llanrinio for two large flood events during calibration (upper pane) and validation (lower pane) periods generated using the RW model calibrated using the Guassian methodology. The shaded area represents the 95 % prediction confidence interval with the solid line the expected value of the predictions. Observed data points are also shown.

HESSD
9, 595–627, 2012